

## PERIODIC TRANSMISSION OF CIRCULAR BINARY FRESNEL ZONE PLATES WITH ETCHING DEPTH AND SUBSTRATE

Yaoju Zhang<sup>1,\*</sup>, Shilei Li<sup>1</sup>, Yan Zhu<sup>1</sup>, Youyi Zhuang<sup>1</sup>, Taikei Suyama<sup>2</sup>, Chongwei Zheng<sup>1</sup>, and Yoichi Okuno<sup>3</sup>

<sup>1</sup>College of Physics and Electronic Information Engineering, Wenzhou University, Wenzhou 325035, China

<sup>2</sup>Akashi National College of Technology, Akashi 674-8501, Japan

<sup>3</sup>Graduate School of Science and Technology, Kumamoto University, Kumamoto 860-8555, Japan

**Abstract**—Based on the scattering theory and the Green function method, a dynamical theory is given for calculating the diffraction of deeply-etched gratings with a stratified structure substrate. The key of our method is that the patterned grating structure is considered as a perturbation to the unpatterned stratified structure rather than to vacuum. Using the first-order Born approximation and in the Fresnel diffraction region, we obtain a simple analytical expression, which can be used to calculating the scattering intensity of deeply-etched circular binary Fresnel zone plates with a stratified substrate (MDECBFZPs). The numerical results show that the focusing intensity at the foci of the MDCBFZP changes periodically with the etching depth and the thickness of the substrate film. Our results are in good agreement with FDTD simulations.

### 1. INTRODUCTION

A Fresnel zone plate (FZP) is an important optical element with light collecting properties and it has many applications in the visible light, millimeter waves, extreme-UV, and x-ray domain regions [1–6]. Many papers based on the Rayleigh-Sommerfeld diffraction integral or on

---

*Received 18 March 2013, Accepted 29 April 2013, Scheduled 19 May 2013*

\* Corresponding author: Yaoju Zhang (zhangyaoju@sohu.com).

the Fresnel diffraction integral analyze the focusing properties of in-plane FZPs [7–10]. Some studies show that the deeply-etched one-dimensional (1-D) gratings have many excellent properties such as high diffraction efficiency [11, 12] and suppressing the sidelobes in the frequency response of a metal-insulator-metal plasmonic filter [13]. The aim of this paper is to analyze the diffraction properties of deeply-etched 2D circular Fresnel zone plates.

Many analysis methods, such as modal method [14], rigorous coupled-wave approach [15], and matrix-method approach [16], are used to calculate the diffraction of deeply-etched 1D periodical gratings. A deeply-etched FZP is a non-periodical structure of grating. It is difficult that above mentioned method is applied to calculate the diffraction of non-periodical gratings. Recently, Kim et al. numerically investigated the transmission optical field enhancement by a metal/dielectric multilayered 2D-focusing sub-wavelength FZP using the 3D finite-difference time-domain (FDTD) method [5]. The FDTD method is appropriate only to the gratings which size are very small, which is difficult to compute the field distribution of a large size FZP. The scattering theory and method is a general method of analyzing the scattering from inhomogeneous media [17], which can be applied to analyze the diffraction of any grating regardless of its size, periodicity or non-periodicity. In 1993, Sammar and André presented a dynamical theory of the diffraction of one-dimensional (1D) ideal deeply-etched stratified Fresnel linear zone plates (SFLZPs) [18, 19], which is based on the scattering theory. Le and Pan applied essentially the method by Sammar and André to calculate the diffraction field of 2D ideal focusing multilayer reflection circular FZPs in 1999 [20]. However, Sammar and André considered the scattering potential of the SFLZP as a perturbation to vacuum in [19]. Obviously, such processing method is only a rough estimation for the diffraction field of the grating without the substrate, because it is more accurate that only the scattering potential of the SFLZP is considered as a perturbation to multilayer structure vacuum. On the other hand, a grating substrate layer is often needed in the actual grating etching. In this paper, we develop the scattering theory to accurately calculate the diffraction of deeply-etched circular binary FZPs with a multilayer substrate film (MDECBFZPs). The key in our method is that scattering potential of the MDECBFZP is considered as a perturbation to multilayer structure rather than to vacuum. We obtain an analytical expression in the first-order Born approximation, which can be easily used to calculate the diffraction field of MDECBFZP in the Fresnel diffraction region.

## 2. INTEGRAL EQUATION FOR THE SCATTERING PROBLEM OF MDEBCFZP

Without loss of generality, let us consider a double-layer optical medium stratified in depth, laterally patterned and referred to the cylindrical frame as shown in Figure 1. The FZP pattern is deeply etched in the upper surface of a double-layer substrate. We assume that the incoming and transmission space are air with the refractive index of  $n_0 = n_3 = 1$ , and the first- and second films are glass and Magnesium fluoride ( $\text{MgF}_2$ ) with the refractive indexes of  $n_2 = 1.52$  and  $n_3 = 1.38$ , respectively. We limit our results to the scalar problem; electromagnetically, it corresponds to the transverse electric ( $TE$ ) polarization incident on the MDECBFZP. The propagation equation is restricted in the patterned stratified structure to the following Helmholtz equation [17]:

$$[\Delta + k^2\varepsilon(\mathbf{R})] U = 0, \tag{1}$$

where  $k = 2\pi/\lambda$  is the wave number,  $\lambda$  is the wavelength, and  $\mathbf{R}$  is the position vector in the scattering medium.  $\varepsilon(\mathbf{R})$  is the dielectric constant of the patterned multilayer structure.

We denote that the dielectric constant of the unpatterned multilayer structure as  $\varepsilon_f(\mathbf{R})$ . It will be convenient to re-write Equation (1) in the form

$$[\Delta + k^2\varepsilon_f(\mathbf{R})] U = V(\mathbf{R})U, \tag{2}$$

where

$$V(\mathbf{R}) = k^2 [\varepsilon_f(\mathbf{R}) - \varepsilon(\mathbf{R})]. \tag{3}$$

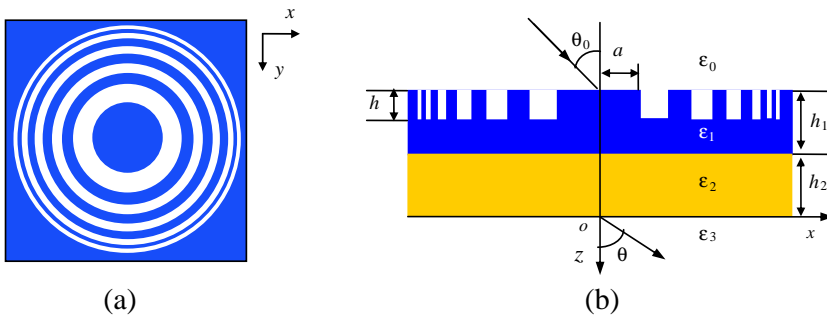


**Figure 1.** Geometry of the scattering of a plane wave incident upon a deeply-etched circular binary Fresnel zone plate with a double-layer substrate: (a) Top down view in  $xy$  plane, and (b) cross-sectional view in  $xz$  plane.

Equation (2) is an inhomogeneous differential equation, where the function  $V(\mathbf{R})$  is called the perturbed scattering potential of the patterned structure relative to the unpatterned stratified structure with the dielectric constant of  $\varepsilon_f(\mathbf{R})$ .

According to the scattering theory [17], Equation (2) can be considered an inhomogeneous differential equation whose general solution is

$$U(\mathbf{r}) = U^{(f)}(\mathbf{r}) + U^{(s)}(\mathbf{r}), \quad (4a)$$

$$U^{(s)}(\mathbf{r}) = -\frac{1}{4\pi} \int_{\Omega} V(\mathbf{R})U(\mathbf{R}) \frac{\exp(ik|\mathbf{r} - \mathbf{R}|)}{|\mathbf{r} - \mathbf{R}|} d\mathbf{R}, \quad (4b)$$

where  $U^{(f)}(\mathbf{r})$  is the total field of the unpatterned multilayer structure and  $U^{(s)}(\mathbf{r})$  is the perturbed scattering field by the patterned grating.  $\Omega$  is the volume in the grating layer.

Assuming that  $r$  is much larger than  $R$  and the thickness of the patterned region is small enough, we expand  $|\mathbf{r} - \mathbf{R}|$  in terms of  $R/r$  and restrict ourselves to the second order in  $R$ . In this case we have the approximation

$$\frac{\exp(ik|\mathbf{r} - \mathbf{R}|)}{|\mathbf{r} - \mathbf{R}|} \approx \frac{\exp(ikr)}{r} \exp(-i\mathbf{k}^d \cdot \mathbf{R}) \exp\left(\frac{ik'R^2}{2r}\right). \quad (5)$$

Here  $\mathbf{k}^d$  is the scattered wave vector, and  $k'$  is related to the angle of  $\tau$  between  $\mathbf{r}$  and  $\mathbf{R}$ ,

$$\mathbf{k}^d = k\mathbf{r}/r, \quad k' = k \sin^2 \tau. \quad (6)$$

On using the approximation (Equation (5)) in the integral in Equation (4b) we see that

$$U(\mathbf{r}) = U^{(f)}(\mathbf{r}) + \frac{\exp(ikr)}{r} f(\mathbf{k}^d, \mathbf{k}, r), \quad (7)$$

and

$$f(\mathbf{k}^d, \mathbf{k}, r) = -\frac{1}{4\pi} \int_{\Omega} V(\mathbf{R})U(\mathbf{R}) \exp(-i\mathbf{k}^d \cdot \mathbf{R}) \exp\left(\frac{ik'R^2}{2r}\right) d\mathbf{R}. \quad (8)$$

### 3. THE FIRST-ORDER BORN APPROXIMATION

For the scattering potential it is clear from Equation (3) that a patterned multilayer structure will scatter weakly if its dielectric constant  $\varepsilon(\mathbf{R})$  differs only slightly from the dielectric constant  $\varepsilon_f(\mathbf{R})$  of the unpatterned stratified structure. In the conventional first-order Born approximation [17], the incident field  $U^{(i)}$  is used to replace the total field  $U$  under the integral in Equation (4b). For the FZP with

a stratified structure substrate, we replace  $U$  under the integral in Equation (4b) with  $U^{(f)}$ , which is a good approximation to the total field. One then obtains, to the solution of the integral equation of scattering, the expression

$$U(\mathbf{r}) = U^{(f)}(\mathbf{r}) - \frac{\exp(ikr)}{4\pi r} \left\{ \int_{\Omega} V(\mathbf{R}) U^{(f)}(\mathbf{R}) \frac{\exp(ik|\mathbf{r} - \mathbf{R}|)}{|\mathbf{r} - \mathbf{R}|} d\mathbf{R} \right\}. \quad (9)$$

This approximate solution is called as the modified first-order Born approximation, or, more precisely, the first-order Born approximation under the circumstances with a stratified structure substrate.

Under the condition of the modified first-order Born approximation and in the Fresnel diffraction region, Equation (8) can be expressed as

$$f(\mathbf{k}^d, \mathbf{k}, r) = -\frac{1}{4\pi} \int_{\Omega} V(\mathbf{R}) U^{(f)} \exp(-i\mathbf{k}^d \cdot \mathbf{R}) \exp\left(\frac{ik'R^2}{2r}\right) d\mathbf{R}. \quad (10)$$

#### 4. SCATTERING OF AN IN-DEPTH STRATIFIED MEDIUM

In this section our purpose is to calculate the optical field distribution ( $U^{(f)}$ ) of an unpatterned multilayer structure. We assume the incident field is a unit-amplitude plane wave,

$$U^{(i)}(\mathbf{r}) = \exp(i\mathbf{k} \cdot \mathbf{r}) = \exp(i\mathbf{k}_{\rho} \cdot \rho) \exp(ik_z z). \quad (11)$$

The Helmholtz equation for an unpatterned multilayer structure can be obtained from Equation (2) as

$$[\Delta + k^2 \varepsilon_f(\mathbf{R})] U^{(f)}(\mathbf{R}) = 0. \quad (12)$$

Let us consider a medium that is laterally unbounded but stratified in depth, that is, the dielectric constant depends only on the  $z$  coordinate. For an arbitrary profile it is possible to divide this profile into homogeneous slabs of thickness  $h_j$ . According to the boundary conditions of the electromagnetic fields, the tangential component of  $U^{(f)}(\mathbf{R})$  is consecutive. Thus the field in the  $j$ th-layer slab can be written as

$$U_j^{(f)}(\mathbf{R}) = \exp(i\mathbf{k}_{\rho} \cdot \rho) U_j^{(f)}(z). \quad (13)$$

where  $U_j^{(f)}(z)$  can be obtained by solving the Helmholtz equation in each homogeneous slab  $j$  of dielectric constant  $\varepsilon_j$ :

$$\left[ \frac{\partial^2}{\partial z^2} + k^2 \varepsilon_j \right] U_j^{(f)}(z) = 0. \quad (14)$$

By using the method presented in [19] we can obtain the scattering field of the unpatterned double-layer structure in the glass

$$U^{(f)} = [T_1 \exp(ik_{1,z}z) + R_1 \exp(-ik_{1,z}z)] \text{rect} \left( \frac{z + h_1 + h_2 - h/2}{h/2} \right) \exp(i\mathbf{k}_\rho \cdot \rho). \quad (15)$$

where  $k_{1,z} = \sqrt{\varepsilon_1 k^2 - k_x^2}$ .

## 5. APPLICATION TO A TRANSMISSION MDECBFZP

### 5.1. Modeling of Transmission Circular Binary Fresnel Zone Plate

We now consider a positive circular binary Fresnel zone plate as shown in Figure 1. The FZP grating is etched in the glass slab of thickness  $h_1$  and the etching depth of the grating is  $h (< h_1)$ . The radius of the central zone is  $a$  and the focal length of the first-order (primary) focus is  $f_1 = a^2/\lambda$ . To enhance the transmission of light, an antireflection layer whose thickness is  $h_2$  is coated on the surface of the glass. The origin  $O$  is chosen at the bottom surface of the antireflection film. The scattering potential of the patterned structure in Equation (3) is expressed as

$$V(\rho, z) = k^2(\varepsilon_b - \varepsilon_a)V_\rho(\rho)V_z(z), \quad (16a)$$

$$V_\rho(\rho) = \sum_{l=0}^L \text{circ} \left[ \rho / \left( a\sqrt{2l+1} \right) \right] - \text{circ} \left[ \rho / \left( a\sqrt{2l} \right) \right], \quad (16b)$$

$$V_z(z) = \text{rect} \left[ (z + h_1 + h_2 - h/2) / (h/2) \right], \quad (16c)$$

By use of the method in [17, 19] we obtain the scattering field of the unpatterned double-layer structure in the glass

$$U^{(f)} = [T_1 \exp(ik_{1,z}z) + R_1 \exp(-ik_{1,z}z)] \text{rect} \left( \frac{z + h_1 + h_2 - h/2}{h/2} \right) \exp(i\mathbf{k}_\rho \cdot \rho). \quad (17)$$

Substituting Equations (16) and (17) into Equation (10), we can calculate the scattering field of the MEDCBFZP with the double-layer substrate. Due to the separability of the electric susceptibility of materials and the etching depth  $h \ll r$ , we can assume a spatial dependence of scattering potential of the scattering medium and calculate the scattering amplitude laterally and in-depth, respectively,

$$f(\mathbf{k}^d, \mathbf{k}, r) = -\frac{1}{4\pi} k^2 (\varepsilon_b - \varepsilon_a) \hat{V}_\rho(k_\rho^d - k_\rho, r) \left[ T_1 \hat{V}_z(k_z^d - k_{1,z}, r) + R_1 \hat{V}_z(k_z^d + k_{1,z}, r) \right]. \quad (18)$$

where

$$\hat{V}_\rho(k_\rho^d - k_\rho, r) = 2\pi \int_0^\infty V_\rho(\rho) \exp\left(\frac{ik\rho^2}{2r}\right) J_0 [(k_\rho^d - k_\rho)\rho] \rho d\rho, \quad (19a)$$

$$\hat{V}_z(k_z^d - k_{1,z}, r) = \int_{-(h_1+h_2)}^{-(h_1+h_2-h)} \exp\left(\frac{ikz^2}{2r}\right) \exp[-i(k_z^d - k_{1,z})z] dz, \quad (19b)$$

$$\hat{V}_z(k_z^d + k_{1,z}, r) = \int_{-(h_1+h_2)}^{-(h_1+h_2-h)} \exp\left(\frac{ikz^2}{2r}\right) \exp[-i(k_z^d + k_{1,z})z] dz. \quad (19c)$$

Due to the etching depth  $h$  much smaller than  $r$ , the Fresnel transform  $\hat{V}_z(q_z, r)$  can be replaced by the Fourier transform  $\tilde{V}_z(q_z)$ . Thus, the total scattering field of the patterned multilayer structure can be simplified as

$$f(\mathbf{k}^d, \mathbf{k}, r) = -\frac{1}{4\pi} k^2 (\varepsilon_b - \varepsilon_a) \hat{V}_\rho(k_\rho^d - k_\rho, r) \left[ T_1 \exp \hat{V}_z(k_z^d - k_{1,z}) + R_1 \hat{V}_z(k_z^d + k_{1,z}) \right]. \quad (20)$$

$\tilde{V}_z(q_z)$  can be easily calculated. The analytical expression of  $\hat{V}_\rho(q_\rho, r)$  at the optical axis (that is, when  $q_\rho = 0$ ) is obtained as

$$\hat{V}_\rho(q_\rho, r) = \pi a^2 \text{sinc}\left(\frac{ka^2}{4r}\right) \exp\left(\frac{ika^2}{4r}(2L+1)\right) \sin\left(\frac{k(L+1)a^2}{2r}\right) / \sin\left(\frac{ka^2}{2r}\right). \quad (21)$$

The positions of the foci from Equation (21) can be obtained as

$$r_j = -\frac{f_1}{2j+1}, \quad j = 0, \pm 1, \pm 2, \dots \quad (22)$$

Applying the Lommel functions we obtain the simple analytical expression of  $\hat{V}_\rho(q_\rho, r)$  for the off-axis case of  $q_\rho \neq 0$ , giving

$$\hat{V}_\rho(q_\rho, r) = \pi a^2 \sum_{m=1}^{2L+1} (-1)^{m+1} u_m, \quad (23a)$$

$$u_m = \begin{cases} \frac{2m}{\xi_m} \exp\left(\frac{i\xi_m}{2}\right) [U_1(\xi_m, \nu_m) - iU_2(\xi_m, \nu_m)], & \xi_m > \nu_m \\ \frac{2mi}{\xi_m} \left[ \exp\left(-\frac{iv_m^2}{2\xi_m}\right) - \exp\left(\frac{i\xi_m}{2}\right) [V_0(\xi_m, \nu_m) - iV_1(\xi_m, \nu_m)] \right], & \xi_m < \nu_m \end{cases}, \quad (23b)$$

where  $U_n$  and  $V_n$  are the Lommel functions [17],  $\xi_m = ma^2k/r$ ,  $\nu_m = \sqrt{maq_\rho}$ .

## 5.2. Numerical Results

In the following calculations, we assume the unit-amplitude plane wave of  $\lambda = 0.65 \mu\text{m}$  is incident on the MDECBFZP along the  $z$  axis of  $\theta_0 = 0^\circ$ . The MDECBFZP's parameters are  $n_0 = n_3 = 1$ ,  $n_1 = 1.5$ ,  $n_2 = 1.38$ ,  $L = 200$ ,  $f_1 = 9 \text{ mm}$ ,  $h_1 = 1.2 \text{ mm}$ ,  $n_2 h_2 = \lambda/4$ , and  $h = \lambda$ . The radius of the FZP is 1.532 mm. Figure 2 shows the scattering intensity ( $I = |f(\mathbf{k}^d, \mathbf{k}, r)|^2$ ) distribution along the  $z$  axis. From the figure it is found that the intensities of each spots are equal for this FZP but their axial full-widths at half-maximum (FWHMs) are unequal, where the axial FWHM of the first-order spot is maximum. Our calculation also shows that the transverse FWHMs of each spots for this FZP are equal in the whole Fresnel diffraction region.

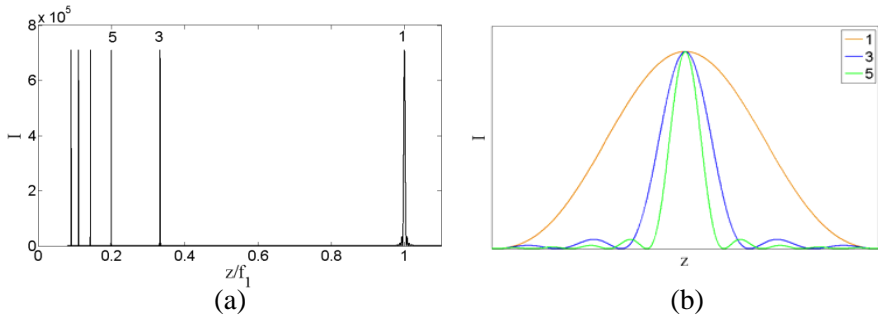


**Figure 2.** Intensity distribution of the scattering light of the MDECBFZP along (a) the optical axis and (b) the comparison of each spot sizes, where 1, 3, and 5 denotes the first-, third-, and fifth-order spots, respectively. The MDECBFZP's parameters are  $n_0 = n_3 = 1$ ,  $n_1 = 1.5$ ,  $n_2 = 1.38$ ,  $L = 200$ ,  $f_1 = 9 \text{ mm}$ ,  $h_1 = 1.2 \text{ mm}$ ,  $n_2 h_2 = \lambda/4$ , and  $h = \lambda$ . The radius of the FZP is 1.532 mm.

Figures 3(a), (b), and (c) show the scattering intensity at the primary focus versus the MDECBFZP's  $h$ ,  $h_1$ , and  $h_2$ , respectively. It is clear that the scattering intensity oscillates periodically. It is found from Figure 3(a) that the scattering intensity is largest when the etched depth  $h$  is equal to odd wavelengths. Our calculation is same as that based on FDTD simulation [5] but different from that in [19]. The result of Sammar and André showed that scattering intensity of the SFLZP increase gradually as the increase of the etching depth of the grating [19]. Therefore, our processing method is necessary to accurately and fast calculating the diffraction field of deeply-etched grating. From Figure 3(c) we find that the scattering intensity can be



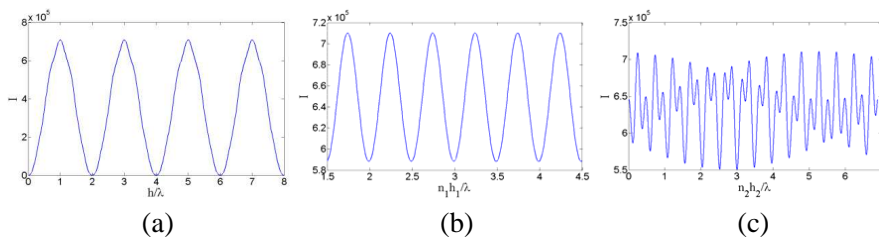


**Figure 3.** The scattering intensity at the primary focus of the MDECBFZP with (a)  $h$ , (b)  $h_1$ , and (c)  $h_2$ . The MDECBFZP’s parameters are same as in Figure 2.

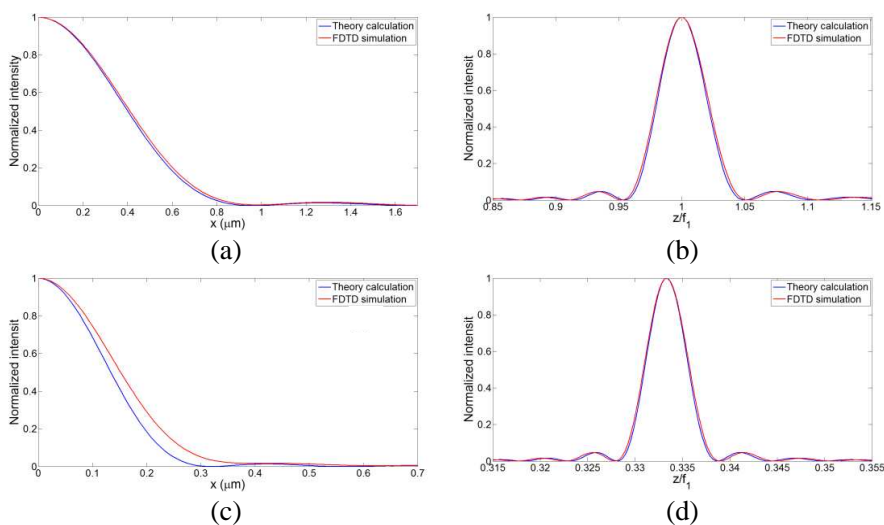


**Figure 4.** Focusing characteristics of a MDECBFZP with  $L = 20$  zones,  $a = 10 \mu\text{m}$ , and  $h = 650 \mu\text{m}$  etching depth under CP illumination. The blue and red curves are the results obtained by the theory formulation and by the FDTD simulation, respectively. (a) and (c) are the transverse intensity distributions in the focus planes of  $z = f_1$  (first-order) and  $z = f_1/3$  (third-order), respectively. (b) and (d) are the axial intensity distribution in the vicinity of the focuses of  $z = f_1$  and  $z = f_1/3$ .

enhanced when the antireflection film has a appropriate thickness. For an example,  $I = 6.455 \times 10^5$  when  $h_2 = 0$  but  $I = 7.09 \times 10^5$  when  $n_2 h_2 = 0.254\lambda$ , the scattering intensity being improved by 9.2% using the antireflection film.

## 6. COMPARISON WITH FDTD SIMULATION RESULTS

With the purpose of validating the model developed on in this paper, we shall compare the previous results with the simulation results provided by the finite-difference time-domain (FDTD) method for the considered FZP. In our FDTD simulations, the input source is a monochromatic circularly-polarized (CP) plane wave with a wavelength  $\lambda = 650$  nm and perfectly matched layer is used as the boundary conditions. The parameters of the MDECBFZP are  $L = 20$  zones,  $a = 10$   $\mu\text{m}$  ( $f_1 = 153.8$   $\mu\text{m}$ ),  $h_1 = h_2 = 10$   $\mu\text{m}$ ,  $n_0 = n_3 = 1$ ,  $n_1 = 1.5$ ,  $n_2 = 1.38$ . Figures 4 and 5 compare the total intensity ( $|E_x|^2 + |E_y|^2 + |E_z|^2$ ) distribution obtained by the theory model and FDTD simulation. From these figures it is seen that the field distribution calculated from the FDTD method is close to that predicted from the analytical model. This implies that the analytical model can match well with FDTD calculation. It is noted that the error between two curves in Figure 4(c) is large at the third-order focus, which may be due to the use of the first-order Born approximation. If the higher-order Born approximation is used, the error is likely reduced.

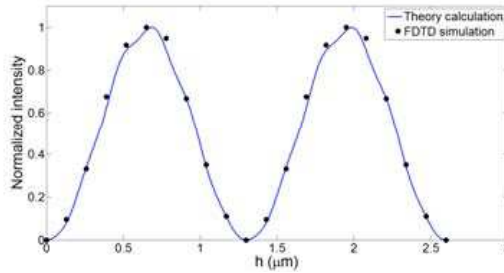


**Figure 5.** The intensity of focusing light at the first-order focus as a function of the etching depth of the MDECBFZP with 20 zones. Solid curve and discrete dots are the results obtained by the theory formulation and by the FDTD simulation, respectively.

## 7. CONCLUSION

Basing on the scattering theory and the Green function method, we have proposed a simple and effective method to calculate the diffraction field distribution of deeply-etched gratings with a stratified structure substrate. The key of our method is that the patterned grating structure is considered as a perturbation to the unpatterned stratified structure rather than to vacuum. As an example, we calculate

the scattering intensity distribution of the transmission MDECBFZP with a double-layer substrate film in the Fresnel diffraction region. The calculation results show that the etched depth and the thickness of each layer in the stratified structure substrate have all an important effect on the scattering intensity at the foci of the MDECBFZP. The diffraction intensity periodically varies with the etching depth of the grating and the thickness of each film in the MDECBFZP. The results deduced from the proposed model shows qualitative agreement with that obtained from the FDTD method. Thus the proposed formulation is useful in simplifying the analysis compared to rigorous diffraction calculations. Although we have focused our attention in the last part of the paper on the MDECBFZP's working by transmission, we must emphasize that our method can be profitably implemented for the reflection FZPs, especially for the FZP's with a high aspect ratio and a multilayer structure substrate. Finally, we have to point out that since we use some approximations in the process of derivation, the obtained analytical formulae for calculating the etched-deeply grating is valid for non-subwavelength gratings and in the Fresnel diffraction region.

## ACKNOWLEDGMENT

This work was supported by the National Natural Science Foundation of China under contract 61078023, the Public Welfare Project of Zhejiang Province science and technology office under contract 2010C31051, and the Natural Science Foundation of Zhejiang Province under contract Y6110505 and Y6090220.

## REFERENCES

1. Baez, A. V., "Fresnel zone plate for optical image formatting using extreme ultraviolet and soft X radiation," *J. Opt. Soc. Am.*, Vol. 51, 405–412, 1961.
2. Schmahl, G., B. Niemann, D. Rudolph, M. Diehl, J. Thieme, W. Neff, R. Holz, R. Lebert, F. Richter, and G. Herziger, "A laboratory X-ray microscope with a plasma X-ray source," *X-Ray Microscopy III*, A. G. Michette, G. R. Morrison, and C. J. Buckley, Eds., Springer-Verlag, Berlin, 1992.
3. Fu, Y., W. Zhou, L. E. N. Lim, C. L. Du, and X. G. Luo, "Plasmonic microzone plate: Superfocusing at visible regime," *Appl. Phys. Lett.*, Vol. 91, 061124, 2007.
4. Mote, R. G., S. F. Yu, B. K. Ng, W. Zhou, and S. P. Lau, "Near-

- field focusing properties of zone plates in visible regime — New insights,” *Opt. Express*, Vol. 16, 9554–9564, 2008.
5. Kim, H. C., H. Ko, and M. S. Cheng, “High efficient optical focusing of a zone plate composed of metal/dielectric multilayer,” *Opt. Express*, Vol. 17, 3078–3083, 2009.
  6. Carretero, L., M. Perez-Molina, S. Blaya, P. Acebal, A. Fimia, R. Madrigal, and A. Murciano, “Near-field electromagnetic analysis of perfect black Fresnel zone plates using radial polarization,” *J. Lightwave Technology*, Vol. 29, 2585–2591, 2011.
  7. Wood, R. W., *Physical Optics*, 3rd Edition, Macmillan, New York, 1934.
  8. Cao, Q. and J. Jahns, “Comprehensive focusing analysis of various Fresnel zone plates,” *J. Opt. Soc. Am. A*, Vol. 21, 561–571, 2004.
  9. Zhang, Y., C. Zheng, and H. Xiao, “Improving the resolution of a solid immersion lens optical system using a multiphase Fresnel zone plate,” *Opt. & Laser Techn.*, Vol. 37, 444–449, 2005.
  10. Zhang, B. and D. Zhao, “Focusing properties of Fresnel zone plates with spiral phase,” *Opt. Express*, Vol. 18, 12818–12823, 2010.
  11. Lu, P., C. Zhou, J. Feng, and H. Cao, “Unified design of wavelength-independent deep-etched fused-silica gratings,” *Opt. Commun.*, Vol. 283, 4135–4140, 2010.
  12. Wang, B., C. Zhou, J. Feng, H. Ru and J. Zheng, “Wideband two-port beam splitter of a binary fused-silica phase grating,” *Appl. Opt.*, Vol. 47, 4004–4008, 2008.
  13. Djabery, R., S. Nikmehr, and S. Hosseinzadeh, “Grating effects on sidelobe suppression in MIM plasmonic filters,” *Progress In Electromagnetics Research*, Vol. 135, 271–280, 2013.
  14. Edee, K., I. Fenniche, G. Granet, and B. Guizal, “Modal method based on subsectional Gegenbauer polynomial expansion for lamellar gratings,” *Progress In Electromagnetics Research*, Vol. 133, 17–35, 2013.
  15. Sun, N.-H., J.-J. Liao, Y.-W. Kiang, S.-C. Lin, R.-Y. Ro, J.-S. Chiang, and H.-W. Chang, “Numerical analysis of apodized fiber Bragg gratings using coupled mode theory,” *Progress In Electromagnetics Research*, Vol. 99, 289–306, 2009.
  16. Francés, F., C. Neipp, A. Márquez, A. Beléndez, and I. Pascual, “Analysis of reflection gratings by a matrix method approach,” *Progress In Electromagnetics Research*, Vol. 118, 167–183, 2011.
  17. Born, M. and E. Wolf, *Principle of Optics*, 7th Edition, Cambridge University Press, Cambridge, 1999.
  18. Sammar, A. and J.-M. André, “Diffraction of multilayer

- gratings and zone plates in the X-ray region using the born approximation," *J. Opt. Soc. Am. A*, Vol. 10, 600–613, 1993.
19. Sammar, A. and J.-M. André, "Dynamical theory of stratified Fresnel linear zone plates," *J. Opt. Soc. Am. A*, Vol. 10, 2324–2337, 1993.
  20. Le, Z. and S. Pan, "Application of quantum scattering theory to 2-D focusing multilayer reflection circular zone plate," *Opt. Commun.*, Vol. 159, 285–292, 1999.